



Short communication

## Experimental simulation of internal short circuit in Li-ion and Li-ion-polymer cells

Wei Cai<sup>a</sup>, Hsin Wang<sup>a,\*</sup>, Hossein Maleki<sup>b</sup>, Jason Howard<sup>b</sup>, Edgar Lara-Curzio<sup>a</sup><sup>a</sup> Oak Ridge National Laboratory, Materials Science and Technology Division, Oak Ridge, TN 37831, USA<sup>b</sup> Motorola Mobility, 1700 Bell Meade Court, Lawrenceville, GA 30043, USA

## ARTICLE INFO

*Article history:*

Received 18 February 2011

Received in revised form 12 April 2011

Accepted 13 April 2011

Available online 21 April 2011

*Keywords:*

Li-ion cells

Li-ion-polymer cells

Internal short circuit

Thermal stability

## ABSTRACT

A multi-parameter controlled pinch test was developed to study the occurrence of internal short circuits in Li-ion and Li-ion-polymer cells. By tuning the control parameters (i.e., cell voltage as well as pinching area, load, and speed), the pinch test can reproducibly create an internal short between a cell jelly-roll's inner layer electrodes as small as 1-mm wide. This recreates conditions similar to those that may occur during service. In this paper we demonstrate the use of the pinch test as a means to assess design and manufacturing changes in Li-ion-polymer cells on their thermal stability and to identify features or characteristics that lower risk of potential thermal events created by internal short circuits.

© 2011 Elsevier B.V. All rights reserved.

### 1. Introduction

Lithium-ion secondary batteries are widely used in portable electronic devices due to their high energy density and long cycle-life. Today's lithium-ion batteries are potentially vulnerable to abuse conditions that might lead to the occurrence of internal short circuit (ISCr), which has been cited as the cause for field incidents and recall of Li-ion batteries [1–3]. ISCr in lithium ion batteries may be caused by physical abuse (drop, crush, etc.) or operational abuse (overcharge by poorly designed charge systems), as well as manufacturing defects (e.g. metallic contaminants, electrode misalignment, etc.). Consequences of ISCr vary with cell design and nature of the event. In most cases ISCr will result only in rapid battery self-discharge, but in rare cases it could trigger the occurrence of thermal runaway [3].

ISCr is an energetic process. Depending on cell design and size of the short-circuit spot, up to 70% of the entire cell energy could be released in less than 60 s [3]. The large amount of energy released around the short spot could result in rapid increases in localized temperature, that if high enough, could trigger thermo-chemical reactions and lead into thermal runaway.

Some studies on thermal stability of Li-ion batteries under ISCr have been carried out. Santhanagopalan et al. examined several ISCr scenarios and found that the short between the lithiated anode material and the cathode aluminum current collector results in

maximum heat generation [4]. They also claimed that the occurrence of thermal runaway is mostly initiated on the anode, and therefore safer design of anodes may further reduce the risk of ISCr. Yamauchi et al.'s study suggests that thermal runaway during a nail penetration test is determined by the total amount of Joule heating produced by the large current due to the ISCr until the discharge of the whole electrode is completed [5]. Barnett et al. modeled thermal performance of 2.2 Ah 18650 cells during ISCr and suggested that local temperature of the short location could be increased by as much as 200 °C, merely due to thermal energy of ISCr [2]. Design of high thermal stability materials and/or materials with slow reaction time may protect Li-ion cells from thermal runaway during ISCr. Kawai's study suggests that lowering electrode–separator interfacial impedance may decrease the risk of thermal runaway during ISCr [6]. Augustin et al. claimed that application of ceramic layer coating on the separator could increase the safety of the Li-ion cells due to the addition of the ceramic coating's contribution of strength and resistance to melting and shrinking of the separator during ISCr [7]. It has been claimed that a composite nonwoven separator composed of a polyacrylonitrile (PAN) nonwoven nano-fiber and ceramic containing nonwoven polyolefin has a higher thermal stability than the conventional microporous membrane separator [8].

Although various test methods have been proposed, there are currently no consensus test methods to assess the thermal performance of lithium-ion cells under ISCr. Existing methods include: forced internal short circuit test developed by the Battery Association of Japan (BAJ) [9], and nail penetration [9–11]. Possible application of small indentation of cell [11,12], and cell pinch tests

\* Corresponding author. Tel.: +1 865 576 5074; fax: +1 865 574 3940.  
E-mail address: [wangh2@ornl.gov](mailto:wangh2@ornl.gov) (H. Wang).

[3] are also being evaluated. The major challenge is the difficulty in reproducibly creating a small, isolated mechanical short circuit in a finished cell to mimic the type of short circuit that is believed to occur during service. Complexity and sample preparation concerns complicate the use of BAJ forced internal short circuit as a standard ISCr test [11,12]. Furthermore, it cannot be applied to lithium-ion polymer cells. For nail penetration and small cell indentation methods, ISCr is likely to be induced in the outermost layers of the cell. Substantial heat can dissipate through the cell-can or the testing nail [3], which is not the most severe case. False results can be produced because of cell construction, i.e. extra metal layers outside the jelly roll. Maleki and Howard have shown a pinch test produces ISCr events inside the jelly roll that are more similar to events that might lead to a failure during service [3]. However this prototype test could not create reproducible, small size internal short ( $\geq 4$  mm short size was produced in [3]) due to lack of accurate control parameters during the test.

In the present work, an improved, automated pinch test method developed jointly by Oak Ridge National Laboratory (ORNL) and Motorola Mobility with various control parameters is introduced. This improved ORNL–Motorola pinch test (1) can reproducibly create  $\sim 1$ – $2$  mm size internal short between two inner electrode layers in the cell; (2) can create different ISCr size by using different control parameters; (3) and it can help distinguish cells with different thermal stability characteristics.

## 2. Experimental setup

Fig. 1(a) and (b) shows a schematic and a photograph of the pinch test setup. The spheres shown in Fig. 1(b) are used to apply concentrated coaxial loading on both sides of a prismatic cell. The spheres are connected with rigid rods to the actuator and load cell of a servohydraulic mechanical testing machine (MTS Systems with model 407 controller). The picture in Fig. 1(b) shows 50.8-mm diameter brass spheres, but tests were carried out with brass and stainless steel spheres of various diameters between 19.1 mm and 50.8 mm. A polycarbonate box was used to contain fragments in case a cell went into thermal runaway during the test and the box was connected to the laboratory's ventilation system. Maleki et al. reported that high-risk ISCr events could be induced consistently when pinching close to the bottom edge of the cell where there is a small gap between the jelly roll and internal wall of the cell-can [3]. Therefore, all test cells in this work were pinched at this location (the center of pinch location is  $\sim 13$  mm away from the edge of cells as shown in Fig. 1(a)). Tests were carried out under a constant displacement rate of the machine's actuator. Mylar tape was used to electrically and thermally insulate cells' aluminum can from the pinching spheres. A K-type thermocouple was taped on the top of the cell to record the cell's surface temperature during the test. The cell open circuit voltage ( $V_{ocv}$ ) was recorded and used as feedback input to a digital controller that controls the operation of the servohydraulic testing machine. Whenever the cell open circuit voltage  $V_{ocv}$  dropped below a preset threshold value, the machine pressing motion was stopped and it was either held at stopped position or returned back to its initial position depending on control program settings. An example of actuator stroke (open circles) and cell  $V_{ocv}$  (solid diamonds) response curves are shown in Fig. 2. In this particular case the control program was set to return mode when the cell voltage dropped below 3.0 V. Note that as the cell  $V_{ocv}$  drops below the 3.0 V threshold, the actuator motion was stopped and quickly returned to its initial position. At the same time the cell  $V_{ocv}$  bounces back to a higher voltage, which indicates that the internal short resistance increases as the mechanical load is withdrawn. Note that there is  $\sim 200$  ms stroke response delay in our current control system, which means that the stroke moves

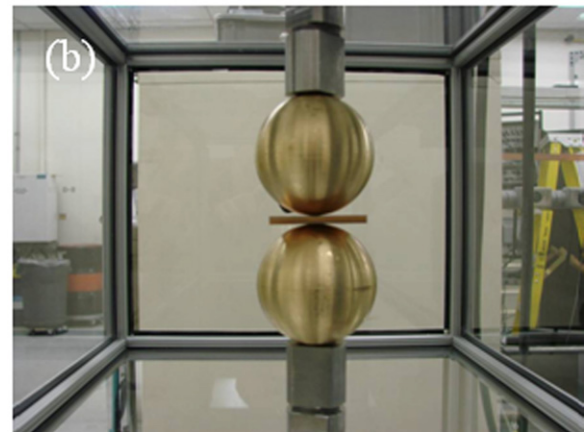
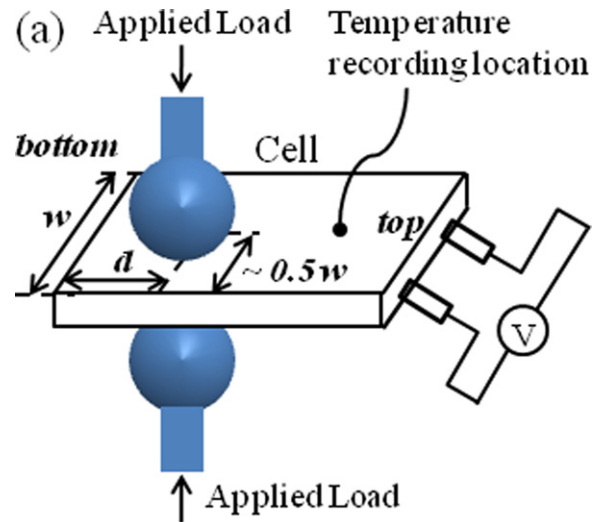


Fig. 1. Schematic (a) and photo image (b) of cell pinch test setup. The distance ( $d$  in (a)) between the center of the pinch location and the bottom edge of the cell is  $\sim 13$  mm. The diameter of the brass spheres in (b) is 50.8 mm. A polycarbonate box was used to contain fragments whenever a cell went into thermal runaway. The box was connected to a ventilation system.

forward  $\sim 2.5 \mu\text{m}$  more after the cell  $V_{ocv}$  drops below the preset threshold voltage.

Various control parameters, such as sphere size, loading speed, stroke response mode (hold or return when the  $V_{ocv}$  of a cell drops below a preset threshold voltage), and the preset threshold volt-

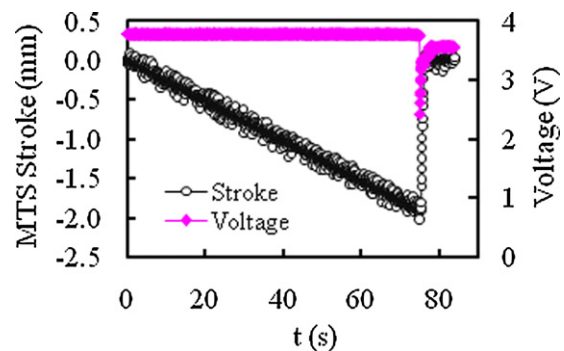


Fig. 2. Example of actuator stroke and cell  $V_{ocv}$  response curves during pinch test. The cell's initial  $V_{ocv}$  was 3.8 V (before test), and the stroke return-voltage was preset at 3.0 V.

**Table 1**  
List of information on prismatic Li-ion and LIP cells used for ISCr tests.

| Cell type | Nominal size:<br>$T \times W \times L^a$ (mm) | Cell mass<br>(g) | Discharge<br>capacity (mAh) | Separator<br>thickness (mm) |
|-----------|---|------------------|-----------------------------|-----------------------------|
| Li-ion A  | 4.3 × 34 × 43                                 | 15.0             | 770                         | 0.018                       |
| LIP B     | 4.5 × 42 × 61                                 | 26.2             | 1500                        | 0.016                       |
| LIP C     | 4.5 × 42 × 61                                 | 26.6             | 1490                        | 0.016                       |

<sup>a</sup>T (thickness), W (width), and L (length).

age, can be adjusted so as to create a repeatable small size ISCr among a few inner layers of a cell's electrodes. Our initial experimental results (as discussed in the following section) indicate that using 25.4-mm diameter stainless steel spheres,  $12.7 \mu\text{m s}^{-1}$  actuator speed, and stroke return mode could reproducibly create small size internal short between the cathode and anode in a few inner layers of the cell. Therefore, the results reported in this article were mostly obtained under these conditions, although ongoing work has been focused on identifying the optimum values of these parameters to create even smaller ISCr short sizes. It is also an open question what the optimum values will be among cells with different design characteristics (size, thickness, can vs. laminate packaging, etc.).

Three different types of cells were tested: prismatic Li-ion A cells, and Li-ion-polymer (LIP) B cells and LIP C cells that have identical construction but different type of separators: LIP B cell uses conventional polyethylene based separator and the LIP C cell uses a specialty separator intended to provide improved thermal stability. All cells have lithium cobalt oxide cathodes and graphite anodes. Information of the test cells' sizes, capacities, and separator thicknesses are listed in Table 1. The cells were first charged to the desired voltage at 0.5 C-rate, followed by charging under a constant voltage until the current dropped below 3% of the rated capacity of the cells.

### 3. Results and discussion

#### 3.1. Internal short size dependence on stroke return-voltage

Other than gross mechanical abuse cases, it is believed that ISCr sizes of about 1 mm (dia.) or smaller could possibly mimic the type of ISCr that occur in the field. There are two possible ways to create such small size ( $\leq 1$  mm) ISCr under the pinch test: (1) use the smallest diameter spheres possible so that only a small part of the cell's separators can be punched through; (2) control the motion of the actuator of the mechanical testing machine to return immediately after the separator is punched through and/or cell shorted (returns the actuator back immediately when a small drop of the cell's  $V_{ocv}$  is detected). Otherwise holes created in the separator would become larger and larger as the actuator continues its pressing motion on the cell.

Fig. 3(a) and (c) shows examples of cell voltage and temperature response curves for stroke return-voltages of 1.0 V and 3.0 V, respectively. The cell with 3.0 V stroke return-voltage reached a lower maximum temperature ( $52^\circ\text{C}$ ) compared to the cell with 1.0 V stroke return-voltage ( $80^\circ\text{C}$ ). Such result suggests creation of a smaller ISCr size and therefore less Joule heating generated in the cell with the higher stroke return-voltage. Also, the cell's final  $V_{ocv}$  for a 3.0 V stroke return-voltage bounces back to a much higher value than that for the case of 1.0 V stroke return-voltage after removing the mechanical load, which again suggests that the higher the stroke return-voltage, the lower the ISCr energy released and the smaller the internal short spot size. Fig. 3(b) and (d) are photos of separators recovered from cells after pinch test with 1.0 V and 3.0 V stroke return-voltages, respectively. Obviously, ISCr occurred in both cases, except that the separator meltdown area is much

**Table 2**  
List of internal short size and maximum cell's surface temperature dependence on stroke return-voltage for ISCr pinch tests on Li-ion A cells. The numbers between parentheses in the last column are the standard deviation about the mean value of the short size for each group of 6 tested cells.

| Cell type | $V_{ocv}$ (V) | Stroke<br>return-voltage<br>(V) | No. of cells<br>tested | Maximum<br>temperature<br>( $^\circ\text{C}$ , mean) | Short size<br>(mm) |
|-----------|---------------|---------------------------------|------------------------|--|--------------------|
| Li-ion A  | 3.8           | 1.0                             | 6                      | 73   | 3.3 (0.6)          |
|           | 3.8           | 2.0                             | 6                      | 60   | 2.2 (0.4)          |
|           | 3.8           | 3.0                             | 6                      | 46   | 1.6 (0.3)          |

smaller for the cell tested with a 3.0 V stroke return-voltage than for the cell tested with a 1.0 V stroke return-voltage.

A summary of results from tests with different stroke return-voltage values are listed in Table 2. The ISCr area contact size of the tested cells was determined based on meltdown size of the separators recovered after pinch tests. During pinch tests with a 3.0 V stroke return-voltage one or two inner layers of the cell anode and cathode were shorted and in most cases that corresponded to the 3rd and/or 4th layer within 12 layers each of anode and cathode electrodes. The test results show that the modified ORNL–Motorola pinch test can create ISCr as small as 1 mm in size by controlling the stroke return-voltage. The average short size from the evaluation of 6 cells with 3.0 V stroke return-voltages was  $\sim 1.6$  mm with the standard deviation of 0.3 mm. These results demonstrate the feasibility of this test method to recreate the type of small size ISCr that may occur during service as a result of:

1. Electrode misalignment that increases risk of anode and cathode touching each other during cell mechanical abuse or drops.
2. Presence of foreign metallic particles within the anode and cathode layers.
3. Presence of burrs on electrodes and tabs created by cutting the metallic components during assembly.

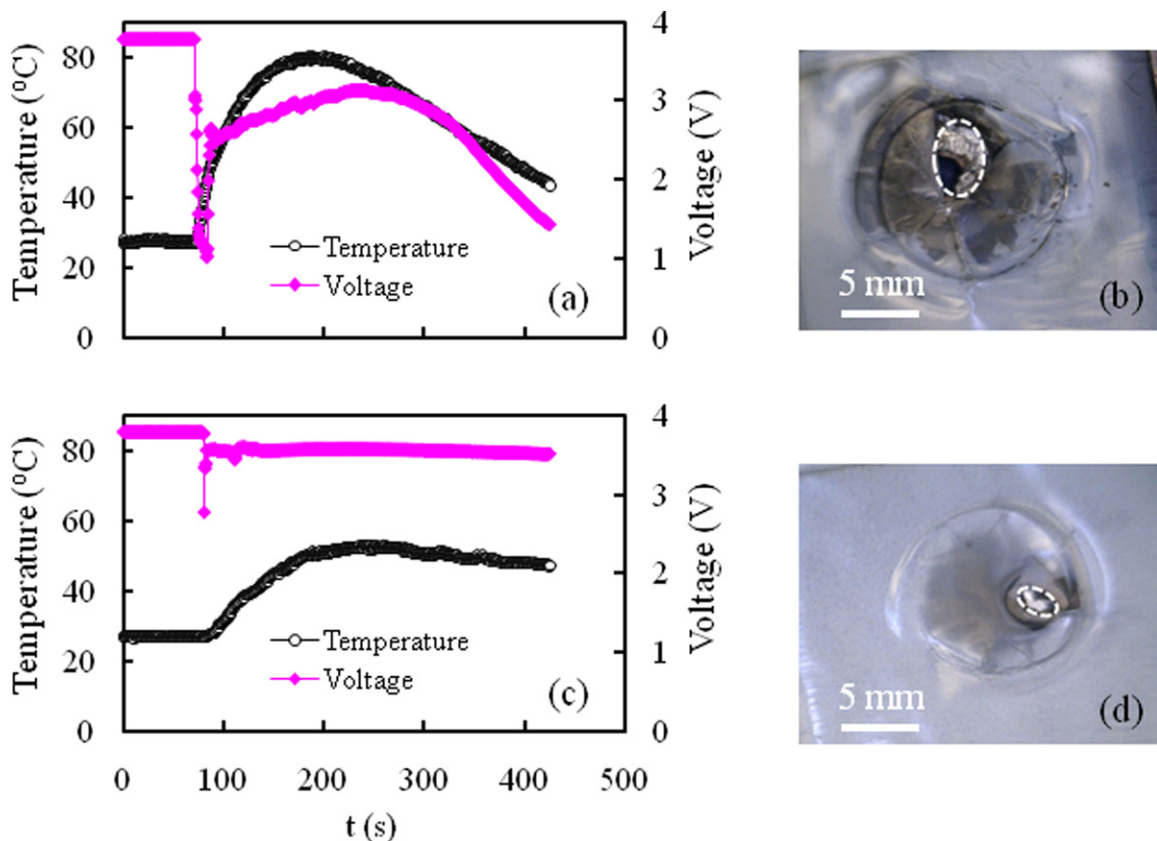
#### 3.2. Risk of thermal runaway during ISCr at different state of charge (SOC)

Table 3 lists values of risk of thermal runaway during ISCr at different state-of-charge (SOC) for prismatic Li-ion A, LIP B, and LIP C cells. 30 prismatic Li-ion A cells at initial  $V_{ocv} = 3.8$  V were first tested with 25.4-mm diameter spheres and different actuator displacement rates ( $12.7 \mu\text{m s}^{-1}$ ,  $25.4 \mu\text{m s}^{-1}$ , or  $101.6 \mu\text{m s}^{-1}$ ), stroke response mode (hold or return), and stroke return-voltage (stroke returns at 1.0 V, 2.0 V or 3.0 V  $V_{ocv}$ ). It was found that using an actuator speed of  $12.7 \mu\text{m s}^{-1}$ , stroke return mode, and stroke return-voltage preset at some voltage just below the cell's initial

**Table 3**  
List of risk of thermal runaway during ISCr at different state of charge for Li-ion A, LIP B and LIP C cells. Different control parameters were used for Li-ion A cells with  $V_{ocv} = 3.8$  V, however the same control parameters were used for Li-ion A cells with  $V_{ocv} \geq 4.0$  V and LIP B and LIP C cells and the stroke returned when  $V_{ocv}$  of the cell dropped 0.3 V below its initial value.

| Cell type | $V_{ocv}$ (V) | Discharge<br>capacity (mAh) | No. of cells<br>tested | No. of thermal<br>runaway cells |
|-----------|---------------|-----------------------------|------------------------|---------------------------------|
| Li-ion A  | 3.8           | 340                         | 30                     | 0                               |
| Li-ion A  | 4.0           | 590                         | 6                      | 0                               |
| Li-ion A  | 4.1           | 680                         | 6                      | 2                               |
| Li-ion A  | 4.2           | 770                         | 6                      | 6                               |
| LIP B     | 3.7           | 160                         | 6                      | 0                               |
| LIP B     | 3.9           | 880                         | 6                      | 0                               |
| LIP B     | 4.0           | 1180                        | 6                      | 6                               |
| LIP C     | 3.7           | 160                         | 6                      | 0                               |
| LIP C     | 4.0           | 1160                        | 6                      | 0                               |
| LIP C     | 4.1           | 1350                        | 6                      | 4                               |
| LIP C     | 4.2           | 1490                        | 6                      | 6                               |





**Fig. 3.** Example temperature and voltage response curves of Li-ion A cells under ISCr with 1.0V (a) and 3.0V stroke return-voltage (c). (b) and (d) show photographs of the corresponding separators recovered from the cells after pinch test. Holes (outlined by white dashed circles) are clearly seen in the separators after ISCr tests. The white regions inside the dashed circle in (b) and (d) are images of electrodes underneath the broken separator. While the dark region inside the dashed circle in (b) is an image of the background (for this case, there is also a hole in the electrode). The cells' initial  $V_{ocv}$  were 3.8 V.

$V_{ocv}$  could produce the most reproducible and smallest ISCr size ( $\sim 1$ – $2$  mm) in a cell with 25.4-mm diameter sphere. Therefore, the rest of the ISCr tests listed in Table 3 were carried-out using 25.4-mm diameter spheres, an actuator speed of  $12.7 \mu\text{m s}^{-1}$ , stroke return mode, and stroke return-voltage preset 0.3 V below the cell's initial  $V_{ocv}$ . None of the 30 cells at initial  $V_{ocv} = 3.8$  V tested went into thermal runaway. Such results show that partially charged Li-ion A cells (at 50% SOC or lower) are very unlikely to reach thermal runaway during mechanical abuse. Table 3 also shows that the risk of thermal runaway during internal short circuit increases with increasing cells' SOC. Compared to prismatic Li-ion A cells, the LIP B cells began to go into thermal runaway during ISCr at a lower charge state (3.9 V; 60% SOC; 880 mAh) than that for the prismatic Li-ion A cell (4.0 V; 76% SOC; 590 mAh). At 4.0 V, failure rate for Li-ion A cells is significantly lower (0 out of 6) than that for the LIP B cells (6 for 6). Results are consistent with an increased risk of thermal runaway with increasing state of charge and cell size. Comparison of the risk of thermal runaway during ISCr for LIP B and LIP C cells will be discussed in detail in the next section.

### 3.3. Case study: assessing the effect of separator on the thermal stability of LIP cells using ISCr pinch tests

All design aspects of LIP B and LIP C cells are identical except for the separator. The LIP C cell specialty separator is designed for higher thermal stability which should offer improved behavior during ISCr. Example of temperature and voltage response curves of LIP B and LIP C cells are shown in Fig. 4(a) and (b), respectively. Here, the initial  $V_{ocv}$  of the two cells were set at 4.0 V, and the stroke return-voltage for both was set at 3.7 V. During ISCr test, the LIP C

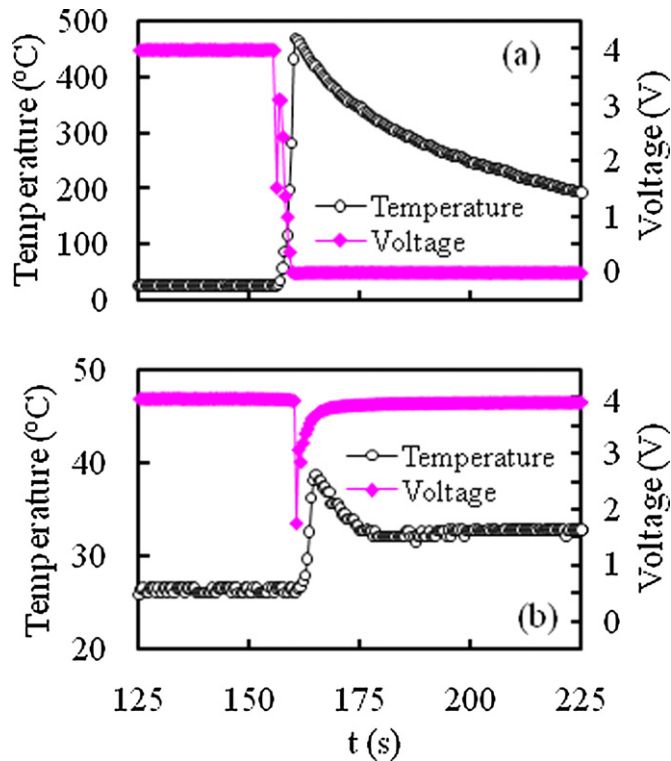


**Fig. 4.** Example temperature and voltage response curves of LIP B (with standard separator) (a) and LIP C (with special separator) (b) during ISCr with initial  $V_{ocv} = 4.0$  V and the stroke return-voltage preset at 3.7 V.

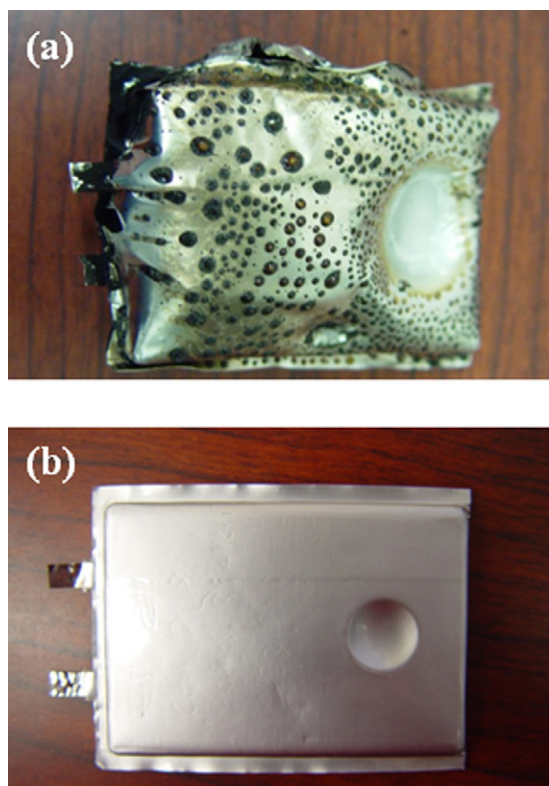


**Fig. 5.** Pictures of LIP B (with standard separator) (a) and LIP C (with special separator), (b) after ISCr tests with initial  $V_{ocv} = 4.0$  V and stroke return-voltage = 3.7 V. Note that the LIP B cell with standard separator (in (a)) went into thermal runaway, however the LIP C cell with special separator (in (b)) did not.

cell's  $V_{ocv}$  bounced back after the mechanical load was removed, its surface temperature increased to 39 °C and no thermal runaway occurred. However the LIP B cell went into full thermal runaway in less than 5 s after the ISCr short was created and the cell's surface temperature exceeded 400 °C. Fig. 5(a) and (b) shows photo images of both cells after pinch tests. The LIP C cell remained intact after the test (Fig. 5b), while the pouch of the LIP B cell was breached and the materials inside the pouch broke down (Fig. 5a). Summary of test results for LIP B and LIP C cells at different SOC are listed in Table 3. For LIP cells charged to 4.0 V (78% SOC; 1160 mAh), all six of the LIP B cells with standard separator and none of the LIP C cells with specialty separator went into thermal runaway. For the LIP C cells, thermal runaway could be induced, but only at higher states of charge (4 out of 6 cells charged to 4.1 V; 91% SOC; 1350 mAh and 6 out of 6 cells charged to 4.2 V; 100% SOC; 1490 mAh). Therefore, LIP C cells with a special separator do offer improved thermal stability relative to the LIP B cells with standard separator. This case study

demonstrates that the pinch test could be used as a test method to evaluate different cell design factors for thermal stability against ISCr events.

#### 4. Conclusions

Systematic ISCr tests on Li-ion A cells, LIP B cells with standard separator, and LIP C cells with specialty separator were carried out using an improved well-controlled pinch test. The improved pinch test can reproducibly create ~1–2 mm size internal short circuit (ISCr) in one or two inner layers of a cell anode and cathode, possibly mimicking the type of internal short circuit that may occur in the field. The induced spot size of the ISCr was found to depend on the stroke return-voltage for a given diameter of the spheres used to apply mechanical loads. The tests also show that the risk of thermal runaway during ISCr increases as the cells' state of charge and capacity increase, which is consistent with a previous report [3]. Moreover, the pinch test could be used to assess the risk of alternate cell designs to thermal runaway and rank them accordingly.

#### Acknowledgements

The authors would like to thank Russ Gyenes (Motorola Mobility) for technical advice, Donald Erdman, Christopher Stevens and Yanli Wang (ORNL) for their help on the pinch tests. This work was sponsored by the Laboratory Directed Research and Development (LDRD) program of ORNL managed by the UT-Battelle LLC, for the Department of Energy under contract DE-AC05000OR22725 and Oak Ridge Associated University through ORISE's postdoctoral research program.

#### References

- [1] J. Zhang, S. Santhanagopalan, P. Ramadass, IMLB-2008 Tianjin China, Abstract 74.
- [2] B. Barnet, D. Ofer, B. Oh, R. Stringfellow, S.K. Singh, S. Sriramulu, IMLB-2008 Tianjin China, Abstract 75.
- [3] H. Maleki, J.N. Howard, J. Power Sources 191 (2009) 568–574.
- [4] S. Santhanagopalan, P. Ramadass, J. Zhang, J. Power Sources 194 (2009) 550–557.
- [5] T. Yamauchi, K. Mizushima, Y. Satoh, S. Yamada, J. Power Sources 136 (2004) 99–107.
- [6] T. Kawai, ECS Conf., Fall 2006, Cancun Mexico.
- [7] S. Augustin, V. Hennige, G. Horpel, C. Hying, Desalination 146 (2002) 23–28.
- [8] T.H. Cho, M. Tanaka, H. Ohnishi, Y. Kondo, M. Yoshikazu, T. Nakamura, T. Sakai, J. Power Sources 195 (2010) 4272–4277.
- [9] Battery Association of Japan, Presentation at UN Informal Working Group Meeting, November 11–13, 2008, Washington, DC.
- [10] J.P. Peres, F. Pertion, C. Audry, Ph. Biensan, A. de Guibert, G. Blanc, M. Broussely, J. Power Sources 97–98 (2001) 702–710.
- [11] Underwriters Laboratories Inc., Presentation at UN Informal Working Group Meeting, November 11–13, 2008, Washington, DC.
- [12] L. Florence, Presentation at Battery Power 2010, Dallas, Texas.